Molecular Microbiology (2013) 90(1), 181–194 ■
doi:10.1111/mmi.12357
First published online 23 August 2013

Triggering sporulation in *Bacillus subtilis* with artificial two-component systems reveals the importance of proper Spo0A activation dynamics

Monika Vishnoi,[1†] Jatin Narula,[2†] Seram Nganbiton Devi,[1] Hoang-Anh Dao,[1] Oleg A. Igoshin[2] and Masaya Fujita[1*]**
[1]*Department of Biology and Biochemistry, University of Houston, Houston, TX 77204-5001, USA.*
[2]*Department of Bioengineering, Rice University, Houston, TX 77030, USA.*

Summary

Sporulation initiation in *Bacillus subtilis* is controlled by the phosphorylated form of the master regulator Spo0A which controls transcription of a multitude of sporulation genes. In this study, we investigated the importance of temporal dynamics of phosphorylated Spo0A (Spo0A~P) accumulation by rewiring the network controlling its phosphorylation. We showed that simultaneous induction of KinC, a kinase that can directly phosphorylate Spo0A, and Spo0A itself from separately controlled inducible promoters can efficiently trigger sporulation even under nutrient rich conditions. However, the sporulation efficiency in this artificial two-component system was significantly impaired when KinC and/or Spo0A induction was too high. Using mathematical modelling, we showed that gradual accumulation of Spo0A~P is essential for the proper temporal order of the Spo0A regulon expression, and that reduction in sporulation efficiency results from the reversal of that order. These insights led us to identify premature repression of DivIVA as one possible explanation for the adverse effects of accelerated accumulation of Spo0A~P on sporulation. Moreover, we found that positive feedback resulting from autoregulation of the native *spo0A* promoter leads to robust control of Spo0A~P accumulation kinetics. Thus we propose that a major function of the conserved architecture of the sporulation network is controlling Spo0A activation dynamics.

Accepted 2 August, 2013. For correspondence. *E-mail mfujita@uh.edu; Tel. (+1) 713 743 9479; Fax (+1) 713 743 8351; **E-mail igoshin@rice.edu; Tel. (+1) 713 348 5502; Fax (+1) 713 348 5877. †These authors contributed equally to this work.

Introduction

Upon nutrient starvation, a majority of *Bacillus subtilis* cells differentiate to produce spores. Extensive studies have elucidated a detailed genetic network of genes involved in an early stage of sporulation (Burbulys *et al*., 1991; Hoch, 1993b; Grossman, 1995; Sonenshein, 2000). At the heart of this network is a phosphorelay (Fig. 1A), in which phosphate is transferred from multiple histidine protein kinases (KinA–E) to a master transcription regulator Spo0A through two intermediate phosphotransferases (Spo0F and Spo0B) (Burbulys *et al*., 1991; Hoch, 1993a; Fawcett *et al*., 2000; Molle *et al*., 2003). Transcriptionally, the phosphorelay genes encoding KinA, Spo0F and Spo0A are controlled by the phosphorylated form of Spo0A (Spo0A~P) directly and indirectly via multiple feedback loops (Fig. 1B). This complex network appears to be the integration point for putative extracellular and intracellular signals that trigger entry into the sporulation programme in response to starvation (Hoch, 1993b; Grossman, 1995).

The initial phase of starvation is marked by a gradual increase in the level of Spo0A~P, which triggers the expression of many genes essential for sporulation (Fujita and Losick, 2003; 2005; Fujita *et al*., 2005). These observations are the motivation for the long-standing hypothesis that sporulation cell-fate can be predicted based on whether or not a cell has a threshold level of Spo0A~P (Hoch, 1993b; Grossman, 1995). We have recently demonstrated that such a Spo0A~P threshold is justified considering the ultrasensitive (switch-like) response of a cascade of feed-forward loops downstream of Spo0A~P (Narula *et al*., 2012). However this Spo0A~P threshold model of cell-fate determination does not explain the experimental observation that rapid accumulation of active Spo0A actually has an adverse effect on sporulation (Fujita *et al*., 2005; Fujita and Losick, 2005). These studies raise two important questions about the mechanistic connection between Spo0A~P dynamics and sporulation cell-fate: (1) Why does accelerated Spo0A~P accumulation impair sporulation efficiency?, and (2) How does the design of the sporulation phosphorelay ensure proper Spo0A~P accumulation dynamics? In this study we took a synthetic biology approach to answer these questions.

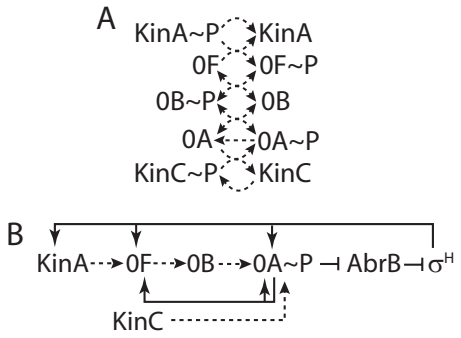

Fig. 1. The sporulation network phosphorelay. Solid arrows and T-shaped bars indicate positive and negative gene regulatory interactions respectively. Dashed arrows indicate phosphotransfer interactions.
A. Post-translational interactions in the wild-type phosphorelay regulatory network. Sensor histidine kinases (KinA and KinC) autophosphorylate and provide phosphate to activate the master regulator Spo0A (0A). KinA transfers phosphate to 0A via Spo0F (0F) and Spo0B (0B), whereas KinC can transfer phosphate to 0A directly.
B. Transcriptional regulatory interactions. Phosphorylated Spo0A (0A~P) becomes a positive regulator for sporulation genes, including those for 0A itself and 0F. 0A~P also indirectly activates the expression of the gene for σ^H, which is essential for sporulation, by repressing AbrB, the repressor of σ^H.

Interrogating naturally occurring networks with methods of synthetic biology has become a widely used approach (Bashor *et al*., 2010; Elowitz and Lim, 2010). The relationships between network architecture and its function can be uncovered more easily by rewiring naturally occurring networks and decoupling interactions or feedback loops than through gene disruption/deletion (Eldar *et al*., 2009; Eswaramoorthy *et al*., 2010; Kuchina *et al*., 2011). We have previously used this approach by building an Artificial Sporulation Initiation (ASI) system in which the phosphate flux of the phosphorelay activating Spo0A is artificially regulated by expressing KinA from an IPTG-inducible promoter (Fujita and Losick, 2005; Eswaramoorthy *et al*., 2010). This system allowed us to uncouple the signal-sensing mechanisms in the phosphorelay from the signal-processing mechanisms and revealed important design properties of the signal processing modules in the sporulation network (Eswaramoorthy *et al*., 2009; 2010; Narula *et al*., 2012).

Here we took this approach further and used novel synthetic networks to control the temporal dynamics of Spo0A~P accumulation. We employed a system in which the kinase KinC is expressed from an IPTG-inducible promoter and Spo0A is expressed from a xylose-inducible promoter. Since KinC can transfer phosphate to Spo0A directly (Kobayashi *et al*., 1995; LeDeaux and Grossman, 1995), both the level of Spo0A and its phosphorylation rate can be easily modulated externally in this system. Using this system, we first determined the relationship between sporulation efficiency and the level of expression of KinC and Spo0A. Surprisingly, we found that sporulation efficiency depends non-monotonically on the levels of these proteins despite the fact that Spo0A activity increases monotonically with increases in Spo0A and KinC. These results were analysed within the framework of a mathematical model. Our modelling showed that only a mechanism coupling the dynamics of Spo0A activation to the cell-fate can explain the impairment of sporulation at high levels of KinC/Spo0A. Further, using a combination of modelling and experiments, we were able to predict and confirm the specific biochemical mechanism underlying the adverse effect of accelerated Spo0A~P accumulation on sporulation in our artificial system. Finally, we modified our inducible KinC-Spo0A and demonstrated that the positive transcriptional feedback in the wild-type phosphorelay is sufficient to ensure proper temporal accumulation of Spo0A~P and efficient sporulation.

Results

KinC-Spo0A artificial two-component system triggers entry into sporulation

To investigate the importance of the dynamics of Spo0A~P accumulation, we perturbed these dynamics artificially. To control the dynamics of accumulation of Spo0A~P we needed to directly control both the level of Spo0A and its phosphorylation rate. To this end, we constructed a strain in which genes for the kinase KinC and Spo0A are independently placed under the control of IPTG-inducible ($P_{hy\text{-}spank}$ for KinC) or the xylose inducible (P_{xylA} for Spo0A) promoters (KinC-Spo0A strain hereafter) (Fig. 2A). We chose KinC (instead of other kinases, such as KinA, etc.) for two reasons. First, it has been previously shown that induced expression of KinC can be used to achieve high sporulation efficiencies irrespective of culture conditions (Fujita and Losick, 2005; see also Supplementary Table S1). Second, since KinC can directly phosphorylate Spo0A, thus bypassing the need for Spo0F and Spo0B (Kobayashi *et al*., 1995; LeDeaux and Grossman, 1995), it offers an easy and direct method of modulating the rate of Spo0A phosphorylation. We also introduced a *spo0F* deletion into this KinC-Spo0A-inducible strain to ensure direct phosphotransfer from KinC to Spo0A. By restricting phosphate flow in this manner and conducting experiments in rich media we were able to minimize the effects of starvation related signals and modulators acting on the phosphorelay.

Using this system we evaluated the effect of different concentrations of IPTG and Xylose (that control the synthesis of KinC and Spo0A respectively) on sporulation efficiency in nutrient-rich conditions. To this end we defined and measured the fraction of total colony-forming units (total cfu = viable cells and spores) that were heat-resistant (heat-resistant cfu = spores; see *Experimental*

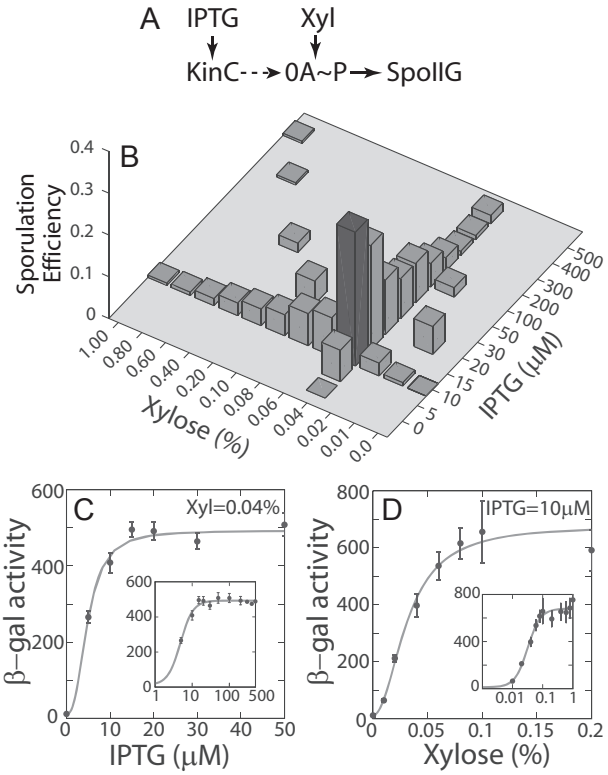

Fig. 2. Simultaneous overproduction of KinC and Spo0A reduces sporulation efficiency.
A. The KinC-Spo0A artificial two-component system (strain MF4317).
B. Bars indicate the results of sporulation efficiency measurements at various combinations of IPTG and xylose inducer concentrations (see *Experimental procedures*). The black bar indicates the optimal combination of IPTG and xylose for sporulation in this strain.
C and D. P_{spoIIG}-*lacZ* reporter was used to measure the effects of KinC and 0A induction on 0A~P levels in the KinC-Spo0A strain.
C. Induction of KinC expression from a $P_{hy\text{-}spank}$ promoter using IPTG leads to a monotonic increase in 0A~P levels (dots and error bars show the mean and standard deviation of three independent measurements of β-galactosidase activity in Miller units).
D. Induction of Spo0A expression from a P_{xylA} promoter using xylose leads to a similar monotonic increase in 0A~P levels (dots). Solid lines in (C) and (D) show Hill-equation fits to the measured responses. Insets in (C) and (D) show the same data on a log-scale for inducer concentrations.

procedures for more details). We found that in the double-induction strain sporulation efficiency depends non-monotonically on the levels of both IPTG and xylose (Fig. 2B): sporulation efficiency was low in the absence of inducers and increased to reach a maximum of about 30% at the optimal combination of 10 μM IPTG and 0.04% xylose (see Fig. 2B). This sporulation efficiency is comparable to that observed in the wild-type cells in sporulation medium (50–70%, Supplementary Table S1). However, our results show that sporulation was impaired by further increasing either the concentration of IPTG or xylose (Fig. 2B and Supplementary Table S2). Going from 10 μM IPTG to 500 μM while keeping xylose at the optimal level of 0.04% decreases sporulation efficiency to ~ 9%. Similarly, going from 0.04% xylose to 1% xylose while keeping KinC induction at the optimal level (at 10 μM IPTG) decreases efficiency to ~ 5%. Moreover, we found that simultaneously overexpressing both KinC and Spo0A by adding excess amounts of two inducers resulted in even greater impairment of sporulation (sporulation efficiency ~ 0.1% at 500 μM IPTG and 1% xylose – Fig. 2B and Supplementary Table S2). Thus, we established an artificial two-component sporulation system (harbouring independently inducible copies KinC and Spo0A) and found that only an optimal combination of Spo0A and KinC expression can be used to trigger an efficient entry into sporulation.

To understand the non-monotonic dependence of sporulation efficiency on IPTG and xylose levels, we quantified the cellular levels of KinC and Spo0A in the KinC-Spo0A strain. We constructed strains expressing a functional KinC-GFP and the wild-type Spo0A under these two inducible promoters respectively. Using this strain, we quantified the amount of KinC and Spo0A proteins at 2 h after the addition of inducers with immunoblot analysis using anti-GFP and anti-Spo0A antibodies respectively. For comparison, the exponentially growing and sporulating cells expressing KinC-GFP from native promoter were cultured in LB and SM media, respectively, and the cell extracts were prepared and quantified with immunoblotting. As shown in Supplementary Fig. S1A, at 10 μM IPTG concentration KinC-GFP levels were approximately fivefold higher than those in the wild-type strain cultured either in rich (LB) or in sporulation (SM) conditions. The Spo0A level at 0.04% xylose was approximately twofold higher than that in the sporulating wild-type strain (Supplementary Fig. S1B). At higher concentrations of the inducers (500 μM IPTG and 1% xylose), the synthesis of KinC and Spo0A proteins was increased further (Supplementary Fig. S1A and B). Thus, the conditions that trigger efficient sporulation correspond to overexpression of both proteins and therefore may not be relevant for wild-type sporulation induction. Nevertheless, the double induction system can enable insights into how level and dynamics of Spo0A~P affect sporulation.

Considering the above results, the low sporulation efficiency seen in our experiments at low IPTG and xylose concentrations (< 10 μM IPTG and < 0.04% xylose) was expected and may be explained by insufficient expression of KinC and/or Spo0A for sporulation. However, the decrease in sporulation efficiency at high inducer concentrations (> 10 μM IPTG and > 0.04% xylose) was somewhat surprising. One possible explanation for this negative effect is that overexpression of KinC and Spo0A with excess IPTG and xylose (> 10 μM IPTG and > 0.04% xylose) may somehow result in a decrease of Spo0A activity, thereby impairing sporulation. To test this, we used

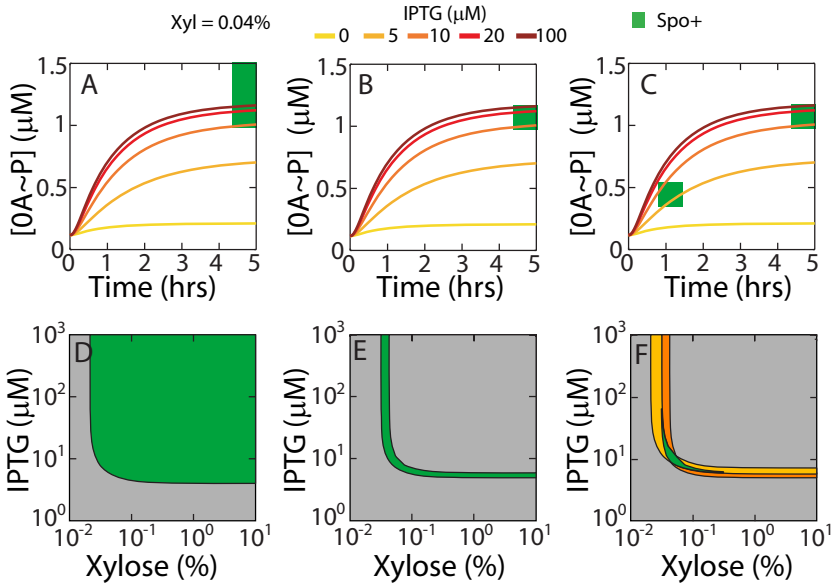

Fig. 3. Dynamic Threshold model explains the dependence of sporulation on IPTG and xylose.
A–C. Dynamics of accumulation of Spo0A~P in the KinC-Spo0A strain at 0.04% xylose and varying IPTG concentrations. Spo0A~P accumulation is sped up by increase in IPTG (KinC expression). Green regions define the Spo0A~P threshold models.
A. Single Threshold: [0A~P] > 0.91 μM at T5.
B. Spo0A~P Range: 0.91 < [0A~P] < 1.1 at T5.
C. Dynamic Threshold: 0.91 < [0A~P] < 1.1 at T5 and 0.46 < [0A~P] < 0.55 at T2.
D–F. Range of IPTG concentrations at for which cells can sporulate as function of the xylose concentration is indicated by green regions. These regions are calculated using Single Threshold (D), Spo0A~P Range (E) and Dynamic Threshold (F) mechanisms respectively. The orange and yellow regions in (F) correspond to the range of IPTG satisfying the constraints 0.91 < [0A~P] < 1.1 at T5 and 0.46 < [0A~P] < 0.55 at T2 respectively.

the P_{spoIIG}-*lacZ* reporter and determined Spo0A activity in this strain at different inducer concentrations. As shown in Fig. 2C and D, in the KinC-Spo0A system, β-galactosidase activity increases monotonically with IPTG and xylose concentrations. Furthermore, we found that the Spo0A activity is higher under conditions of simultaneous overexpression of both KinC and Spo0A (500 μM and 1% xylose), as compared with the optimal conditions for sporulation (10 μM IPTG and 0.04% xylose; see Supplementary Table S2). Therefore, the impairment of sporulation by the induced overexpression of KinC and Spo0A is not due to a decrease in Spo0A activity.

Mathematical modelling identifies the role of Spo0A~P accumulation kinetics in efficient sporulation

To understand how simultaneous overproduction of both KinC and Spo0A impairs sporulation, despite an increase in Spo0A activity, we constructed a mathematical model of the KinC-Spo0A artificial two-component system. In our model the parameters for the expression of KinC and Spo0A from the inducible promoters $P_{hy\text{-}spank}$ and P_{xylA} respectively, were constrained using immunoblotting measurements of KinC and Spo0A protein levels and the single-cell measurements of transcriptional reporters $P_{hy\text{-}spank}$-*yfp* and P_{xyl}-*cfp* (see Supplementary Methods and Supplementary Fig. S2). The post-translational interactions in the model include KinC autophosphorylation, direct phosphorylation of Spo0A by KinC and dephosphorylation of Spo0A by the Spo0E phosphatase.

The results of deterministic simulations of our model showed that increasing the concentration of IPTG from 10 to 500 μM to increase KinC levels accelerates the accumulation of Spo0A~P (Fig. 3A–C). The modelling results also showed that increasing Spo0A levels by increasing xylose concentration from 0.04% to 1% leads to a similar acceleration in Spo0A~P dynamics (Supplementary Fig. S3).

We combined these results with phenomenological thresholds for Spo0A~P levels to determine how the decrease in sporulation during simultaneous overproduction of KinC and Spo0A can be explained. Three types of Spo0A~P threshold mechanisms were used:

(1) **Single Threshold:** For sporulating cells, Spo0A~P concentration at steady state must be above some threshold level (a_1) (our simulations indicate that Spo0A~P reaches steady state at 5 h after induction, hereafter T5), i.e. a_1 < [Spo0A~P] at T5.
(2) **Spo0A~P Range:** For sporulating cells, Spo0A~P concentration at steady state must be greater than some level (a_1) but below another threshold (a_2), i.e. a_1 < [Spo0A~P] < a_2 at T5.
(3) **Dynamic Thresholds:** For sporulating cells, the steady-state (T5) concentration of Spo0A~P must be greater than a_1 but less than a_2 and greater than b_1 but less than b_2 at the point of asymmetric septation (T2, 2 h after induction in our conditions), i.e. a_1 < [Spo0A~P] < a_2 at T5 and b_1 < [Spo0A~P] < b_2 at T2.

These thresholding mechanisms, although phenomenological, represent different cell-fate decision mechanisms and can be used to discriminate between different hypotheses regarding the mechanistic basis of decisions during sporulation. The Single Threshold mechanism (#1 as above) is the traditional model (Bischofs *et al.*, 2009; Levine *et al.*, 2012) used to predict sporulation outcomes.

It assumes that cells only need to achieve a minimum Spo0A~P level to sporulate. The dynamics of Spo0A~P accumulation do not affect the sporulation outcome in this case. The dynamics are also irrelevant to the outcome of the Spo0A~P Range mechanism (#2 above). However, under this thresholding mechanism, excess Spo0A~P at steady state can prevent sporulation. Finally, in the Dynamic Threshold mechanism (#3 above), sporulation decision depends on Spo0A~P levels at two time points. As a result, cell-fate is determined not only by the Spo0A~P level achieved but also by the rate of accumulation of Spo0A~P. We applied these thresholding mechanisms to the results of our deterministic simulations to determine which combination of IPTG and xylose concentrations would allow sporulation. As shown in Fig. 3D–F, these three thresholding mechanisms make qualitatively distinct predictions about the range of inducer concentrations that allow sporulation (green regions indicate inducer concentrations where cells sporulate according to criteria listed above). The Single Threshold mechanism (#1) predicts that there exists a minimum IPTG and xylose concentration for successful sporulation and any IPTG and xylose concentration above these minimum levels leads to sporulation (see green region in Fig. 3D). The Spo0A~P Range mechanism (#2) predicts that there exists a range of IPTG concentrations for successful sporulation and that this range depends on the level of xylose (green region in Fig. 3E). The Dynamic Thresholds mechanism (#3) combines two such xylose-dependent IPTG ranges (orange and yellow regions indicate inducer concentrations where $a_1 < [Spo0A\sim P] < a_2$ at T5 and $b_1 < [Spo0A\sim P] < b_2$ at T2 respectively; Fig. 3F). As a result, the dynamic thresholding mechanism (#3) predicts that there is an optimal combination of IPTG-xylose concentrations for triggering sporulation efficiently. We note that the regions of inducer concentrations where sporulation can occur (green regions in Fig. 3D–F) are distinctly shaped for the three models. The shape of each region is robust to the exact values of the thresholds used or of their time points. Comparing these results with Fig. 2B we found that *only* the Dynamic Thresholds mechanism (#3) can explain the experimentally demonstrated relationship between sporulation efficiency and the inducer concentrations (compare Fig. 3F and Fig. 2B). Therefore, entry into sporulation depends on both the Spo0A~P level and the dynamics of Spo0A~P accumulation in a fashion similar to that suggested by the Dynamic Thresholds mechanism (#3). In addition, these results also suggest that the impairment of sporulation by overproduction of KinC and Spo0A is the result of premature activation of Spo0A, as trajectories corresponding to these conditions overshoot the T2 threshold from above (Fig. 3C). We concluded that premature induction of high levels of Spo0A at the earlier time point may impair sporulation, and began to explore the possible molecular mechanism(s) underlying this effect.

Accelerated accumulation of Spo0A~P perturbs the temporal order of Spo0A regulon expression

The Dynamic Thresholds mechanism used in the previous section explains the effect of overproduction of KinC and Spo0A by assuming that accelerated Spo0A~P accumulation impairs sporulation. To justify this assumption and validate the Dynamic Thresholds mechanism mechanistically, we examined the effects of accelerated Spo0A~P accumulation on the induction and repression of genes in the Spo0A regulon.

Based on the known network architecture of the Spo0A regulon, we predicted two consequences of the accelerated accumulation of Spo0A~P: (1) no effect on the indirectly controlled, low Spo0A~P threshold genes (Fig. 4A, left panel), and (2) premature activation/repression of the directly controlled high Spo0A~P threshold genes (Fig. 4A, right panel). The first consequence mainly refers to genes that are indirectly activated by Spo0A~P through the repression of AbrB and the resulting derepression of σ^H (Fujita *et al*., 2005). The kinetics of activation of these genes is determined mainly by dilution and degradation rate of AbrB and thus Spo0A~P is not rate-limiting. Therefore, the indirectly controlled low-threshold genes in the Spo0A regulon are independent of Spo0A~P accumulation rate. In contrast, in the latter case, we expected that the accelerated accumulation of Spo0A~P could activate/repress the Spo0A-directly controlled high-threshold genes in a premature fashion, resulting in the abnormal control of low threshold (indirect) and high threshold (direct) events in the sporulation gene expression programme.

To test these predictions, we extended our mathematical model of the KinC-Spo0A system from the previous section to include Spo0A regulated genes. In this extended model, two types of Spo0A~P regulated genes were included: (1) directly activated/repressed high threshold genes: *spoIIGB* (the second gene in a *spoIIG* operon encoding pro-σ^E, the precursor of σ^E, hereafter SpoIIGB) and *divIVA* (encoding DivIVA involved in cell division site selection), and (2) an indirectly activated low threshold gene *citG* (encoding σ^H-controlled fumarate hydratase gene) (Fig. 4A) (Molle *et al*., 2003; Fujita *et al*., 2005). It should be noted that even though we use these specific Spo0A~P target genes, our results reflect the effects of perturbations on the temporal expression of low- and high-threshold genes in general.

Results of deterministic simulations of this model showed that simultaneous overproduction of KinC and Spo0A by increasing inducer concentrations to 500 μM IPTG and 1% xylose (solid curves Fig. 4B) from 10 μM

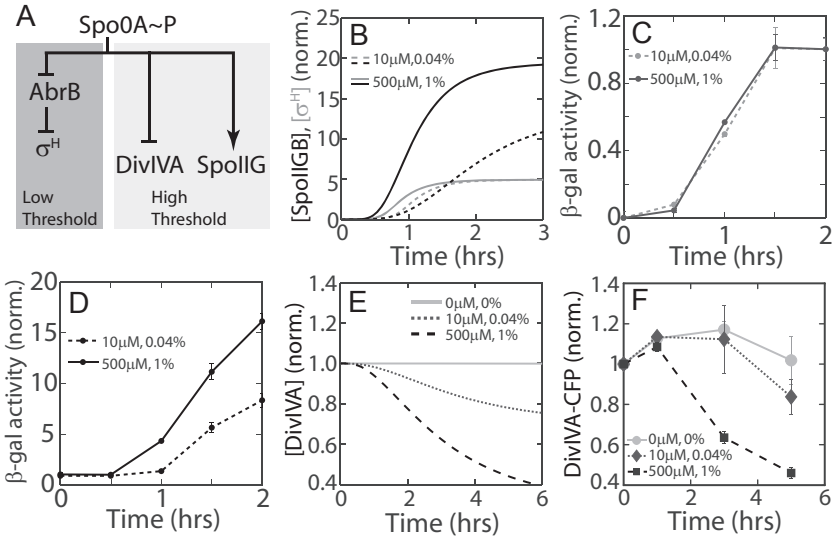

Fig. 4. Rapid Spo0A~P accumulation reverses the temporal order of low and high threshold genes.
A. Two types of gene expression control exerted by Spo0A~P: direct activation/repression of high threshold genes (*spoIIG/divIVA*) and indirect activation of genes like σ^H by relieving repression by AbrB.
B. Accumulation dynamics of directly and indirectly activated Spo0A targets (SpoIIGB – black curves, σ^H – grey curves) in the KinC-Spo0A strain as predicted by our model. Two different conditions are shown: 10 μM IPTG, 0.04% xylose (solid) and 500 μM IPTG, 1% xylose (dashed). Note that higher inducer concentrations shift the onset of [SpoIIGB] accumulation to an earlier time point but do not significantly affect [σ^H] accumulation.
C and D. Accumulation of σ^H (C) and transcription of *spoIIG* (D) in the KinC-Spo0A strain were measured every 30 min after induction using P_{citG}-*lacZ* and P_{spoIIG}-*lacZ* reporters respectively. In both (C) and (D), points on dashed and solid curves indicate measurements for 10 μM IPTG, 0.04% xylose and 500 μM IPTG, and 1% xylose respectively. β-Galactosidase activity (Miller units) was normalized to the level at T2 (C) and T0 (D) respectively after subtracting appropriate background.
E. Predicted dynamics of a directly repressed Spo0A target DivIVA in the KinC-Spo0A strain under conditions of no inducer (solid curve), 10 μM IPTG, 0.04% xylose (dotted curve) and 500 μM IPTG, and 1% xylose (dashed curve).
F. Level of DivIVA was assayed with immunoblotting in the KinC-Spo0A strain expressing a DivIVA–CFP fusion protein (MF4812) at 0 μM IPTG, 0% xylose (circles), 10 μM IPTG, 0.04% xylose (diamonds) and 500 μM IPTG, 1% xylose (squares) at indicated time points (see Supplementary Fig. S4). DivIVA–CFP measurements were divided by the immunoblot measurements of constitutively expressed σ^A and then normalized by the T0 values in each case.
Error bars show the standard deviation of three independent measurements at each time point.

IPTG and 0.04% xylose (dashed curves Fig. 4B) accelerates the accumulation of Spo0A~P, resulting in the early expression of the Spo0A-directly activated *spoIIGB* gene (black curves in Fig. 4B). Furthermore, our simulations show that the increases in both KinC and Spo0A have no significant effect on the response profile of the σ^H-regulated *citG* gene that is indirectly regulated by the low threshold level of Spo0A~P (Fig. 4B – grey curves).

To verify these modelling results, we experimentally measured gene expression profiles of the low- and high-threshold Spo0A-regulated genes in the KinC-Spo0A strain. For the measurement of the expression of the low-threshold Spo0A indirectly regulated and the high-threshold Spo0A directly controlled genes, β-galactosidase activities from a σ^H controlled *citG* P2 promoter (Tatti *et al*., 1989) and a Spo0A controlled *spoIIG* operon promoter (Fujita *et al*., 2005) fused to the *lacZ* gene (P_{citG}-*lacZ* and P_{spoIIG}-*lacZ*) were separately assayed. The results indicated no significant effect on the response profile of the σ^H-regulated gene expression (Fig. 4C) despite the accelerated accumulation of Spo0A~P, which is evident from the premature activation of the high threshold P_{spoIIG}-*lacZ* reporter (Fig. 4D). Our model also predicted that accelerated Spo0A~P accumulation resulting from overproduction of KinC and Spo0A causes the earlier onset of reduction in the expression of high threshold Spo0A-directly repressed genes such as *divIVA* (Fig. 4E). To verify this experimentally we measured the protein level of endogenous DivIVA using immunoblotting for a functional DivIVA–CFP fusion protein (Patrick and Kearns, 2008; Eswaramoorthy *et al*., 2011) in the KinC-Spo0A strain (MF4812). We found that, in contrast to the optimum conditions of 10 μM IPTG and 0.04% xylose (dotted curve in Fig. 4F), DivIVA expression at T3 is significantly reduced under conditions of overproduction of KinC and Spo0A (500 μM IPTG and 1% xylose; see dashed curve in Fig. 4F and Supplementary Fig. S4).

We conclude that these experimental results agree with the mathematical modelling, thus confirming our prediction that overproduction of KinC and Spo0A reverses the

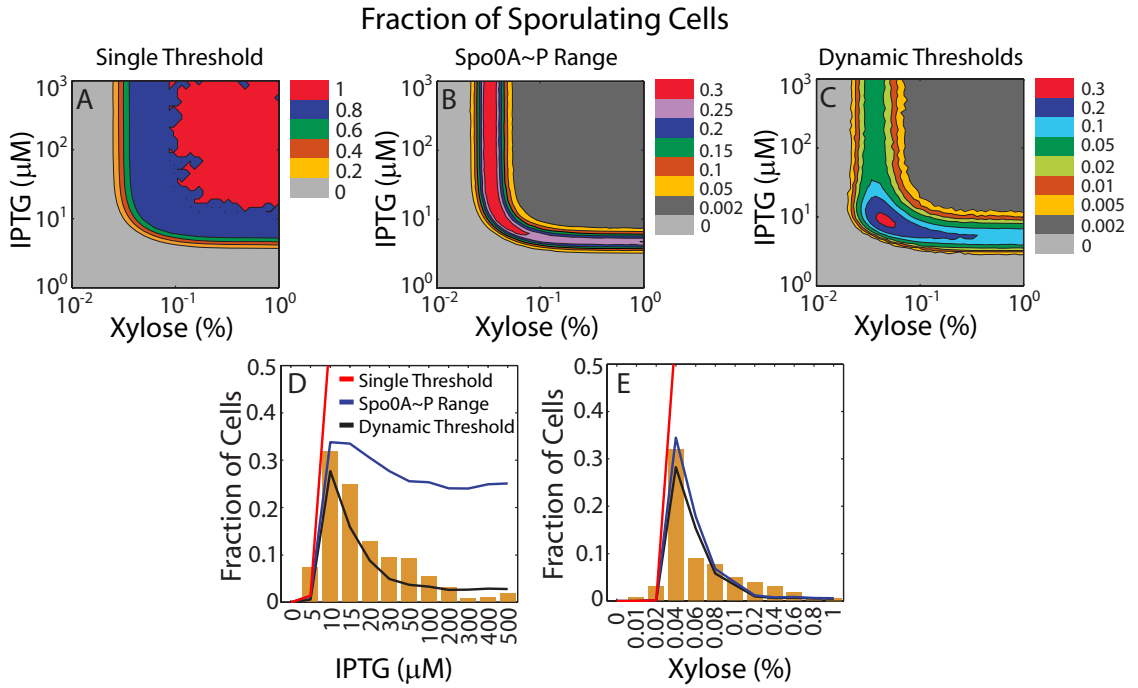

Fig. 5. Dynamic Threshold model explains the existence of optimal IPTG and xylose concentrations for sporulation.
A–C. Contour diagrams of fraction of sporulating cells as predicted by using Single Threshold (A), Spo0A~P Range (B) and Dynamic Thresholds (C) mechanisms on stochastic simulation results. Single Threshold: [IIGB] > 13.5 μM at T5. Spo0A~P Range: [IIGB] > 13.5 μM and [DivIVA] > 0.84 μM at T5. Dynamic Threshold: [IIGB] > 13.5 μM and [DivIVA] > 0.84 μM at T5 and [IIGB] > 2 μM and [DivIVA] > 0.97 μM when $[\sigma^H] = 0.8$. Note that only the Dynamic Thresholds mechanism predicts that the sporulating fraction reaches its optimum at 10 μM IPTG and 0.04% xylose.
D and E. Comparison of model predicted sporulating fraction and experimentally measured sporulation efficiencies. Bars indicate the results of sporulation efficiency measurements at various combinations of IPTG and xylose inducer concentrations (same data as Fig. 2B).
Xylose = 0.04% in (D) and IPTG = 10 μM in (E). The lines show the fraction of sporulating cells predicted by using the Single Threshold (red), Spo0A~P Range (blue) and Dynamic Threshold (black) on the trajectories from stochastic simulations of the KinC-Spo0A model.

regular temporal order of expression of the Spo0A regulon: *spoIIG* expression increases and DivIVA is repressed significantly before σ^H activation.

These results can be used to provide a mechanistic basis for the Dynamic Thresholds mechanism. As indicated in the previous section, according to the Dynamic Thresholds mechanism, sporulating cells must have $a_1 < [\text{Spo0A}\sim\text{P}] < a_2$ at T5 and $b_1 < [\text{Spo0A}\sim\text{P}] < b_2$ at T2. The minimum Spo0A~P thresholds a_1 and b_1 can be explained by the requirement for the high-threshold Spo0A~P-activated genes like *spoIIGB*. Accordingly, the minimum Spo0A~P threshold may be replaced by the requirements $c_1 < [\text{SpoIIGB}]$ at T5 and $d_1 < [\text{SpoIIGB}]$ at T2. Furthermore, if we assume that there are minimum threshold concentrations for high-threshold Spo0A~P repressed genes like *divIVA*, the upper bounds on Spo0A~P threshold (a_2 and b_2) can be replaced by lower bounds on DivIVA as: $c_2 < [\text{DivIVA}]$ at T5 and $d_2 < [\text{DivIVA}]$ at T2. Moreover since σ^H accumulation rate is robust to changes in Spo0A~P accumulation kinetics, σ^H can be used as a time-keeping device in this strain. As a result, evaluating the requirements of $d_1 < [\text{SpoIIGB}]$ and $d_2 < [\text{DivIVA}]$ at a specific concentration of σ^H is equivalent to evaluating these requirements at a fixed time point. Taken together, the three types of Spo0A~P thresholding mechanisms can then be reformulated as: Single Threshold: $[\text{SpoIIGB}] > c_1$ at T5 (steady state); Spo0A~P Range: $[\text{SpoIIGB}] > c_1$ and $[\text{DivIVA}] > c_2$ at T5; and Dynamic Thresholds: $[\text{SpoIIGB}] > c_1$ and $[\text{DivIVA}] > c_2$ at T5 and $[\text{SpoIIGB}] > d_1$ and $[\text{DivIVA}] > d_2$ when $[\sigma^H] = s_0$.

To validate these mechanisms, we performed stochastic simulations of the KinC-Spo0A model using the Gillespie SSA algorithm. In the stochastic simulations of our model, cellular responses at the single-cell level are characterized by noisy trajectories. To separate these trajectories into sporulating and non-sporulating phenotypes, we apply the three threshold models described above and calculate the fraction of cells that sporulate at each inducer condition. The values of the thresholds c_1, c_2, d_1 and d_2 were chosen by optimizing the fit of the Dynamic Thresholds mechanism to the experimentally measured sporulation efficiencies (see Fig. 5 and Supplementary Information).

As expected from the results in Fig. 3, our stochastic simulations show that only the Dynamic Thresholds mechanism predicts that the fraction of sporulating cells is maximal at 10 μM IPTG and 0.04% xylose (compare Fig. 5A–C and Fig. 2B). Moreover, the sporulating fraction predicted by the Dynamic Thresholds mechanism matches the experimentally observed non-monotonic dependence of sporulation efficiency on IPTG and xylose concentrations (Fig. 5D and E). The combination of mathematical modelling and experimental results suggests that a minimal threshold concentration of each of the proteins at two different time points is required for a successful entry into sporulation.

Accelerated Spo0A~P accumulation leads to premature repression of DivIVA which impairs chromosome segregation

The thresholds for DivIVA can be explained by the essential requirement for this protein during sporulation. In the early phase of sporulation, accumulation of σ^H leads to asymmetric septation by promoting increased expression of FtsZ (Gholamhoseinian *et al.*, 1992). DivIVA plays an important role around this time since it is essential for proper chromosome segregation; *divIVA* mutants have impaired chromosome segregation, which leads to formation of chromosome-free compartments and poor sporulation efficiency (Thomaides *et al.*, 2001; Soufo *et al.*, 2008). Based on these facts, we reasoned that early repression of DivIVA in conditions of KinC and Spo0A overexpression may mimic the phenotype of *divIVA* mutants, resulting in the low sporulation efficiency due to lack of the proper chromosome segregation during sporulation.

To evaluate the effect of Spo0A and KinC overexpression on DivIVA levels and on chromosome segregation in single cells, we performed fluorescence microscopy experiments with a functional DivIVA–CFP fusion construct (Eswaramoorthy *et al.*, 2011). We found that DivIVA–CFP levels in single cells were significantly lower at 500 μM IPTG and 1% xylose compared with 10 μM IPTG and 0.04% xylose (Fig. 6A). Moreover, DivIVA–CFP was irregularly localized in the cells under the high inducer conditions (Supplementary Fig. S5). Further, using DAPI (4-,6-diamidino-2-phenylindole dihydrochloride) to stain for DNA, we found that, in approximately 35% of the cells, DNA was improperly segregated at 500 μM IPTG and 1% xylose as compared with approximately 8% at 10 μM IPTG and 0.04% xylose (Fig. 6B–G and Supplementary Fig. S6). Thus, our results suggest that low sporulation efficiency under conditions of overproduction of KinC and Spo0A in the artificial two-component system could be explained at least in part by the improper chromosome segregation, resulting from premature repression of DivIVA.

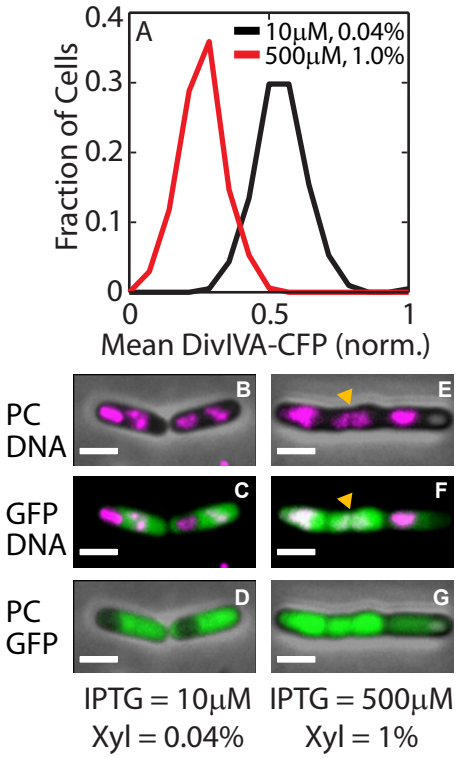

Fig. 6. Overproduction of KinC and Spo0A results in early repression of DivIVA and improper chromosome segregation.
A. Histograms for DivIVA levels at T2 after the addition of 0.04% xylose and 10 μM IPTG (black) and 1% xylose and 500 μM IPTG (red). DivIVA level in single cells was measured by expressing a functional DivIVA–CFP fusion in the KinC-Spo0A strain. DivIVA–CFP fluorescence levels were normalized to the maximum level seen in both conditions.
B–G. The KinC-Spo0A strain harbouring a *gfp* reporter gene under the control of the *spoIIG* promoter and stained with DAPI for DNA was cultured in the presence of (B–D) 0.04% xylose and 10 μM IPTG; and (E–G) 1% xylose and 500 μM IPTG and examined with fluorescence microscopy. Typical cells under each condition are shown. GFP and DAPI (DNA) are pseudo-coloured with green and magenta respectively. Yellow carats indicate cells with improper chromosome segregation. PC, phase-contrast image. Scale bar: 2 μm.

Autoregulation of spo0A ensures proper temporal co-ordination of high and low threshold gene expression

Thus far, our results show that the impairment of sporulation by rapid accumulation of Spo0A~P can be explained by the premature repression of its targets such as DivIVA before σ^H is fully activated. We also noted that in the wild-type phosphorelay the σ^H-mediated positive feedback to *spo0A* may limit the accumulation of Spo0A~P until σ^H is fully activated. Taking all this into account we hypothesized that putting *spo0A* under native promoter may be sufficient to ensure proper Spo0A~P dynamics and prevent premature activation/repression of the Spo0A regulon.

To test this hypothesis, we first constructed a mathematical model for a strain where KinC is expressed from

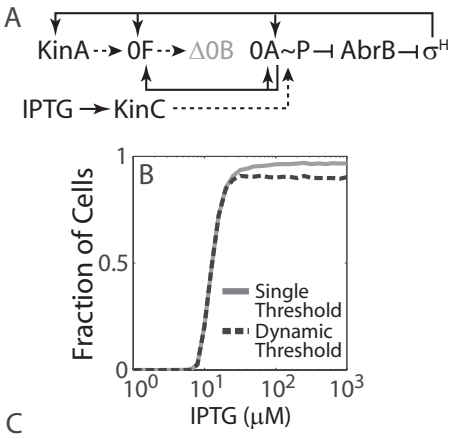

C

KinC Δ*spo0B*			
IPTG (μM)	cfu/ml		Sporulation Efficiency
	Viable cells	Spores	
0	6.6×10^8	1.9×10^4	2.8×10^{-5}
10	5.7×10^8	1.4×10^8	2.4×10^{-1}
500	9.5×10^7	8.2×10^7	8.6×10^{-1}

Fig. 7. σ^H-mediated feedback prevents decrease in sporulation efficiency at high KinC levels.
A. KinC induction strain with *spo0B* deletion and *spo0A* expressed from native promoter (MF4419).
B. Predicted fraction of sporulating cells as a function of IPTG in this strain. Fraction of cells that sporulate in this strain was calculated using the results of stochastic simulations at different IPTG concentrations and the Single Threshold (grey curve) and Dynamic Thresholds (black dashed curve) models. The [SpoIIGB] and [DivIVA] thresholds used are the same as Fig. 5. Predictions based on the Dynamic Thresholds model are largely equivalent to predictions based on a single [SpoIIGB] threshold (Single Threshold model) for this strain.
C. Results of sporulation efficiency measurements at various concentrations of IPTG in the KinC induction strain harbouring *spo0B* deletion mutation (MF4419). Note that sporulation efficiency increases with IPTG.

the IPTG inducible $P_{hy\text{-}spank}$ promoter, *spo0A* is regulated by its native promoters, and the phosphotransferase *spo0B* is deleted to ensure only direct phosphotransfer from KinC to Spo0A (*Δspo0B*, Fig. 7A). The expression of *spo0A* is regulated by multiple Spo0A binding sites that regulate both σ^A-dependent and σ^H-dependent promoters (Chastanet and Losick, 2011). Thus native *spo0A* regulation results in direct feedback from Spo0A to itself (both positive and negative loops) and indirect positive feedback via σ^H. Deterministic simulations of this model showed that increase in KinC expression can lead to earlier onset of the high Spo0A~P threshold programme (*spoIIGB* activation and *divIVA* repression; Supplementary Fig. S7), similar to the KinC-Spo0A strain. However, the autoregulation of *spo0A* expression ensures that this onset does not precede the activation of σ^H (Supplementary Fig. S7). Consequently, sufficient levels of high threshold repressed genes like DivIVA are always available at the appropriate time point in the sporulation programme (Supplementary Fig. S7).

The results of stochastic simulations (Fig. 7B) for this strain showed that the fraction of sporulating cells predicted based on the Dynamic Thresholds mechanism (black dashed line) increases monotonically with IPTG concentration. These predictions are very similar to the fraction of sporulating cells computed based on the Single Threshold mechanism (grey solid line). Therefore, the fraction of sporulating cells in this strain is mainly limited by the requirements for activation of high-threshold genes (such as *spoIIGB*). The increase in sporulation efficiency at higher IPTG concentrations can then be explained as more cells achieving sufficiently high Spo0A~P level (Fig. 7B and Supplementary Fig. S7). Moreover, σ^H accumulation always precedes the repression of the high threshold genes (such as DivIVA), and as a result, sufficient levels of these proteins are available for normal cellular functions ([DivIVA] ≥ 0.97 μM when [σ^H] = 0.8 μM; see Fig. 7B and Supplementary Fig. S7).

Next we computationally examined the roles of the individual autoregulatory feedbacks in Spo0A~P accumulation by removing either the negative direct feedbacks or both positive and negative direct feedbacks from Spo0A to itself. Our results showed that the indirect σ^H-mediated positive feedback to *spo0A* alone is capable of ensuring the gradual accumulation of sufficient levels of Spo0A~P required for sporulation (Supplementary Fig. S7). These results agree with the observations of Chastanet and Losick (2011) who showed that the elimination of all Spo0A binding sites from the *spo0A* promoters does not hamper sporulation.

To verify these predictions, we experimentally constructed this strain (MF4419, Fig. 7A) and examined how sporulation depends on the level of KinC. We tested for sporulation efficiency in LB media in the presence of varying concentrations of IPTG. As expected from our modelling results, we found that with *spo0A* under its native promoter, sporulation efficiency at 500 μM IPTG was significantly higher (9×10^{-1}) than that in the KinC-Spo0A strain (10^{-2}) at high 500 μM IPTG and 1% xylose (compare Fig. 7C and Supplementary Table S2).

Taken together these results suggest that σ^H-mediated positive feedback to *spo0A* transcription in the sporulation phosphorelay is sufficient to ensure proper timing of activation/repression of high-threshold genes with the sporulation programme.

Discussion

We have constructed a genetically engineered strain that decouples and rewires the sporulation phosphorelay

network thereby establishing an artificial two-component system of sporulation comprising KinC and Spo0A. In contrast to the previously reported systems (Fujita and Losick, 2005; Eswaramoorthy *et al*., 2010; Chastanet *et al*., 2011), our artificial two-component system offers unique control over the kinetics of Spo0A~P accumulation and thus is a powerful tool to investigate why Spo0A~P accumulation needs to be gradual for efficient sporulation.

We found that at a certain combination of Spo0A and KinC protein expression levels (10 μM IPTG and 0.04% xylose, Fig. 2B), Spo0A~P gradually accumulated to high enough levels so that cells sporulate efficiently. However, increases in KinC or Spo0A expression beyond this condition can significantly speed-up the rate of Spo0A~P accumulation, shift the onset of high threshold gene expression to earlier time points, and as a result, decrease sporulation efficiency (500 μM IPTG and/or 1% xylose, Fig. 2B).

These experimental results can be explained using mathematical modelling: the onset of increase/decrease in expression of high threshold activated/repressed genes (such as *spoIIG* and *divIVA* respectively) is shifted to earlier time points by overproduction of KinC or Spo0A (Fig. 4). This shift of the timing of high threshold gene expression events is especially significant considering that the dynamics of indirect targets of Spo0A~P, such as σ^H and its controlled genes, are not affected by KinC or Spo0A overproduction (Fig. 4B and C). In fact, experimentally, at the optimal combination of Spo0A and KinC induction, high threshold gene expression is initiated after the onset of σ^H activation whereas σ^H is activated after the onset of the expression of high threshold genes if Spo0A and/or KinC are overproduced (Fig. 4B–D). As a result, the accelerated accumulation of Spo0A~P reverses the temporal order of the sporulation gene expression programme. We hypothesize that this change in temporal order of the sporulation gene expression programme has an adverse effect on sporulation efficiency because repression of essential genes occurs abnormally early.

Several genes repressed by Spo0A~P are involved in cell division, DNA replication, cell-shape determination and protein synthesis (Molle *et al*., 2003; Fujita *et al*., 2005; Eswaramoorthy *et al*., 2011). Thus, overproduction of KinC and Spo0A in the artificial two-component system could cause abnormalities in cell division, DNA replication and protein synthesis, and as a result, adversely affect sporulation. Among the genes repressed by Spo0A~P, *divIVA* may be the most obvious candidate to explain the importance of proper timing. Although it is repressed during sporulation, DivIVA plays an important role in chromosome segregation in the early phase of sporulation (Thomaides *et al*., 2001; Wu and Errington, 2003). In conditions of Spo0A and KinC overexpression, *divIVA* is repressed prematurely (Fig. 4E and F), resulting in improper chromosome segregation and increased incidence of chromosome-free compartments (Fig. 6 and Supplementary Figs S5 and S6). Similar phenotypes have been observed in sporulation-defective *divIVA* mutants (Thomaides *et al*., 2001). Thus, premature repression of DivIVA could at least partially explain our observation of decreased sporulation efficiency in conditions of high KinC and Spo0A expression. As *divIVA* is repressed at high levels of Spo0A~P (Fujita *et al*., 2005), gradual accumulation of Spo0A~P in the wild-type strain under starvation conditions ensures that it is repressed only after it has served its function during the early phase of sporulation – a period which also includes the activation of low-threshold genes such as σ^H by Spo0A~P (Fujita *et al*., 2005).

We also found that simultaneous overproduction of KinC and Spo0A results in swollen cell morphologies and changes the staining pattern of cell membranes with lipophilic fluorescent dye, FM4-64 (Supplementary Fig. S5). The swollen morphologies may be explained by the early repression of a gene *mreB*. This gene is repressed (indirectly) by high levels of Spo0A~P during sporulation (Fujita *et al*., 2005) and is responsible for cell shape determination as a prokaryotic homologue of actin (Defeu Soufo and Graumann, 2005; Formstone and Errington, 2005). The abnormal staining pattern of the membrane can be attributed to inappropriate fatty acids synthesis, since Spo0A~P has been shown to control fatty acids synthesis and maintain membrane lipid homeostasis during early stages of sporulation (Pedrido *et al*., 2013). Thus accelerated and inappropriate activation of Spo0A appears to have pleiotropic effects on various cellular functions. However, the mechanism by which these resulting aberrant morphologies could interfere with sporulation remains unclear.

The artificial induction KinC-Spo0A two-component system demonstrates the importance of gradual accumulation of Spo0A~P. To explain how the structure of the phosphorelay network plays a role in ensuring gradual Spo0A~P accumulation we put these results in a broader context. In principle, there could be two mechanisms to slow-down Spo0A~P accumulation during the onset of sporulation: (1) limit the phosphate flux that activates Spo0A and (2) limit the amount of Spo0A available for activation.

Chastanet *et al*. (2011) and more recently Levine *et al*. (2012), found that overexpressing σ^H, Spo0F and Spo0A had little effect on the dynamics of Spo0A~P accumulation whereas overexpressing of KinA and KinC speeds up sporulation. Based on these results, it was concluded that Spo0A~P accumulation during starvation is limited by the phosphate flux (i.e. mechanism 1). However, accumulation of Spo0A activity can be made even faster by artifi-

cially inducing the expression of the constitutively active mutant form of Spo0A: Spo0A-sad67. But with induced expression of Spo0A-sad67 cells sporulate poorly (Fujita and Losick, 2005) whereas kinase overexpression strains sporulate efficiently (Fujita and Losick, 2005; de Jong *et al*., 2010; Eswaramoorthy *et al*., 2010; Chastanet *et al*., 2011; Levine *et al*., 2012; Narula *et al*., 2012). This indicates that Spo0A activation in kinase overexpression strains may be slower than that in the Spo0A-sad67 induction strain. Thus mechanism (2) may prevent Spo0A~P from accumulating too quickly when kinase is overproduced.

Our experiments with the inducible strains reported here concur with the importance of mechanism (2) in modulating Spo0A activation. Results for KinC-Spo0A induction strains indicate that kinase overexpression strains are limited by the amount of Spo0A available for activation. The simultaneous overproduction of both Spo0A and KinC can overcome this limitation and further speed up Spo0A activation and thereby reduce sporulation efficiency. However, the high sporulation efficiency of KinC induction strain with native *spo0A* promoter (Fig. 7) suggests that the Spo0A feedback loops ensure gradual Spo0A~P accumulation. Notably, feedback architecture is a common feature of many phosphorelays (Williams *et al*., 2005; Williams and Cotter, 2007) and may thus represent a common strategy for proper dynamical control in variety of functional settings.

How does Spo0A autoregulation ensure gradual Spo0A~P accumulation? Positive feedback is known to slow-down response dynamics (Savageau, 1976) and our modelling results suggest that the σ^H-mediated positive feedback from Spo0A to itself is sufficient to ensure that high and low threshold Spo0A~P targets are expressed in the proper order for sporulation (Fig. 7 and Supplementary Fig. S7). Additional direct positive and negative feedback loops emerging from Spo0A~P binding to its promoters may provide further control over of Spo0A~P accumulation dynamics. Alternatively, these loops may affect other aspects of the phosphorelay response such as sensitivity to kinase expression or even to act as amplifiers of noise (Chastanet *et al*., 2011).

Conclusions and perspectives

Our novel genetic systems provide a unique opportunity to obtain insight into the functional role of the phosphorelay in sporulation. Using these systems we have found that the σ^H-mediated positive feedback in the phosphorelay network is not absolutely required for efficient sporulation, but plays a crucial role under conditions when phosphorylation flux is no longer limited. We conclude that the complex architecture of the phosphorelay includes several redundant mechanisms that ensure proper dynamic execution of the sporulation programme under a variety of conditions.

Experimental procedures

Strains, plasmids and oligonucleotides

All strains for experiments were derived from the *B. subtilis* prototrophic strain PY79 (Youngman *et al*., 1985). Details of strains used in this study are listed in Supplementary Table S4 in the supplementary material. The strain harbouring the *divIVAΩlinker-cfp* was a gift from Prahathees Eswaramoorthy and Kumaran S. Ramamurthi. All plasmid constructions (Supplementary Table S5) were performed in *Escherichia coli* DH5α using standard methods. The oligonucleotide primers used for plasmid construction are listed in Supplementary Table S6.

Media and culture conditions

To induce the synthesis of the protein of interest in *B. subtilis* cells, an isopropyl-β-D-thiogalactopyranoside (IPTG)-inducible *hyper-spank* promoter ($P_{hy\text{-}spank}$) (Fujita and Losick, 2005) and/or a xylose-inducible promoter (P_{xylA}) (Gueiros-Filho and Losick, 2002; Wagner *et al*., 2009) were used (kind gifts from D. Rudner, Harvard Medical School). The inducer (IPTG and/or xylose) was added at the indicated concentration to the culture in LB medium during the exponential growth phase (optical density at 600 nm, 0.5). Sporulation of the wild-type strain was induced by the procedure of the resuspension method (Sterlini and Mandelstam, 1969).

Sporulation efficiency and β-galactosidase assays

Sporulation efficiency was determined in overnight (16–18 h) culture, as cfu per ml (spores) after heat treatment by incubation at 80°C for 10 min, compared with cfu per ml (viable count) of the pre-heat treatment sample. Assays of β-galactosidase activity were performed as described previously (Eswaramoorthy *et al*., 2009).

Immunoblot analysis

For KinC-GFP, cells of the KinC strain (a gene for KinC is placed under the control of an IPTG-inducible $P_{hy\text{-}spank}$ promoter) harbouring *kinC-gfp* (MF2734) were cultured to mid-exponential phase ($OD_{600} = 0.5$) in LB, and IPTG was added at indicated concentrations. Cells were harvested at 2 h after induction. Cells of the wild-type strain harbouring *kinC-gfp* (MF2659) were cultured the same as above, except for the IPTG addition, as nutrient rich conditions. Cells of MF2659 were cultured in hydrolysed casein (CH) growth medium and resuspended in Sterlini & Mandelstam (SM) medium as sporulation conditions (Sterlini and Mandelstam, 1969). For Spo0A, the KinC-Spo0A strain (MF4318, a gene for KinC is placed under the control of an IPTG-inducible $P_{hy\text{-}spank}$ promoter and a gene for Spo0A is placed under the control of a xylose-inducible P_{xylA} promoter) was cultured as above, and xylose was added at

indicated concentrations. MF2659 was used for the wild-type Spo0A protein. Cell extracts for immunoblot analysis were prepared from 2 h after IPTG addition in LB or 2 h culture in SM medium by sonication. Immunoblot analysis was performed as described previously (Fujita and Losick, 2002). Polyclonal anti-GFP (Rudner and Losick, 2002), anti-Spo0A (Fujita, 2000) and anti-σ^A (Fujita, 2000) antibodies were used to detect corresponding proteins or GFP-tagged proteins. The intensities of each band after immunostaining were quantified with a FluorChem digital imaging system (Alpha Innotech). σ^A was served as an internal standard control for normalization (Fujita, 2000). The protein levels were normalized to both the levels of σ^A and then the levels of each of the corresponding proteins in the wild-type strain (MF2659).

Fluorescence microscopy

Fluorescence microscopy was performed as described previously (Eswaramoorthy *et al.*, 2009). The membrane and DNA were stained with FM4-64 and DAPI (4′, 6-diamidino-2-phenylindole) respectively. Image acquisition and analysis were performed with Slidebook (Intelligent Imaging Innovations). Single cell fluorescence intensities (arbitrary pixel units) were quantified using MicrobeTracker Suite (Sliusarenko *et al.*, 2011) and custom MATLAB code.

Mathematical modelling

Our model focused on the KinC-Spo0A two-component system and the dynamics of Spo0A~P and its targets in the KinC-Spo0A double induction strain (MF4318) and the Δ*spo0B*, $P_{hy\text{-}spank}$-kinC induction strain (MF4419). SpoIIGB and DivIVA were included in the model as examples of high threshold activated and high threshold repressed genes respectively. σ^H was included as an example of an indirectly activated low threshold gene. We assumed that in both strains KinC directly phosphorylates Spo0A and that KinC was the sole kinase capable of activating Spo0A, as the activities of KinA and KinB under rich-media conditions are negligible. For the double induction strain, the transcription of Spo0A and KinC depended on the xylose and IPTG concentrations respectively. Appropriate transcription rates for these promoters as a function of inducer concentration were determined from the results of the immunoblotting experiments described above and previously reported measurements of Spo0A and KinC concentrations. For the native *spo0A* promoter in the MF4419 strain, we modelled the rate of transcription v_{spo0A} as a Hill-function dependent on both Spo0A~P and σ^H concentrations:

$$v_{spo0A} = k_v \frac{1}{1+[0A\sim P]^2/K_1^2} + k_s \frac{[\sigma^H]}{K_H+[\sigma^H]} \frac{1+f_A[0A\sim P]^2/K_3^2}{1+[0A\sim P]^2/K_3^2+[0A\sim P]^2/K_2^2}$$

Here k_v and k_s represent the transcription rates for *spo0A* from the vegetative and sporulation-specific promoters P_v and P_s respectively. K_H represents the binding affinity for σ^H. K_1, K_2 and K_3 represent the binding affinities for the three Spo0A~P binding sites in Spo0A promoter. f_A represents the fold change in gene expression effected by binding of Spo0A~P to site 3 in the Spo0A promoter. Transcription rates for all target genes are similarly modelled with Hill-functions and binding affinities based on the results in Fujita *et al.* (2005). The details of post-translational phosphorylation/dephosphorylation reactions as well as all parameter values used are provided in the supplementary information. The *ode45* solver of MATLAB was used for deterministic simulations of the model, and the Gillespie algorithm in COPASI was used for all stochastic simulations.

Acknowledgements

We thank Daniel Kearns, Prahathees Eswaramoorthy and Ashlee Eswara for comments and valuable discussions. We are especially grateful for the strains kindly provided by D. Rudner, P. Eswaramoorthy and Kumaran S. Ramamurthi. The authors are also grateful to Benjamin B. Mull and Brooke A. Gowl for their editing suggestions, This work was supported by National Science Foundation (awards MCB-0920463, MCB-1244135 and MCB-1244423) as well as by the Norman Hackerman Advanced Research Program (003652-0072-2007) to M.F. and HHMI International Student Research Fellowship to J.N.

References

Bashor, C.J., Horwitz, A.A., Peisajovich, S.G., and Lim, W.A. (2010) Rewiring cells: synthetic biology as a tool to interrogate the organizational principles of living systems. *Annu Rev Biophys* **39:** 515–537.

Bischofs, I.B., Hug, J.A., Liu, A.W., Wolf, D.M., and Arkin, A. (2009) Complexity in bacterial cell–cell communication: quorum signal integration and subpopulation signaling in the *Bacillus subtilis* phosphorelay. *Proc Natl Acad Sci USA* **106:** 6459–6464.

Burbulys, D., Trach, K.A., and Hoch, J.A. (1991) Initiation of sporulation in *B. subtilis* is controlled by a multicomponent phosphorelay. *Cell* **64:** 545–552.

Chastanet, A., and Losick, R. (2011) Just-in-time control of Spo0A synthesis in *Bacillus subtilis* by multiple regulatory mechanisms. *J Bacteriol* **193:** 6366–6374.

Chastanet, A., Vitkup, D., Yuan, G.C., Norman, T.M., Liu, J.S., and Losick, R.M. (2011) Broadly heterogeneous activation of the master regulator for sporulation in *Bacillus subtilis*. *Proc Natl Acad Sci USA* **107:** 8486–8491.

Defeu Soufo, H.J., and Graumann, P.L. (2005) *Bacillus subtilis* actin-like protein MreB influences the positioning of the replication machinery and requires membrane proteins MreC/D and other actin-like proteins for proper localization. *BMC Cell Biol* **6:** 10.

Eldar, A., Chary, V.K., Xenopoulos, P., Fontes, M.E., Loson, O.C., Dworkin, J., *et al.* (2009) Partial penetrance facilitates developmental evolution in bacteria. *Nature* **460:** 510–514.

Elowitz, M., and Lim, W.A. (2010) Build life to understand it. *Nature* **468:** 889–890.

Eswaramoorthy, P., Guo, T., and Fujita, M. (2009) *In vivo* domain-based functional analysis of the major sporulation

sensor kinase, KinA, in *Bacillus subtilis*. *J Bacteriol* **191:** 5358–5368.
Eswaramoorthy, P., Duan, D., Dinh, J., Dravis, A., Devi, S.N., and Fujita, M. (2010) The threshold level of the sensor histidine kinase KinA governs entry into sporulation in *Bacillus subtilis*. *J Bacteriol* **192:** 3870–3882.
Eswaramoorthy, P., Erb, M.L., Gregory, J.A., Silverman, J., Pogliano, K., Pogliano, J., and Ramamurthi, K.S. (2011) Cellular architecture mediates DivIVA ultrastructure and regulates Min activity in *Bacillus subtilis*. *Mbio* **2:** e00257-00211.
Fawcett, P., Eichenberger, P., Losick, R., and Youngman, P. (2000) The transcriptional profile of early to middle sporulation in *Bacillus subtilis*. *Proc Natl Acad Sci USA* **97:** 8063–8068.
Formstone, A., and Errington, J. (2005) A magnesium-dependent *mreB* null mutant: implications for the role of *mreB* in *Bacillus subtilis*. *Mol Microbiol* **55:** 1646–1657.
Fujita, M. (2000) Temporal and selective association of multiple sigma factors with RNA polymerase during sporulation in *Bacillus subtilis*. *Genes Cells* **5:** 79–88.
Fujita, M., and Losick, R. (2002) An investigation into the compartmentalization of the sporulation transcription factor sigmaE in *Bacillus subtilis*. *Mol Microbiol* **43:** 27–38.
Fujita, M., and Losick, R. (2003) The master regulator for entry into sporulation in *Bacillus subtilis* becomes a cell-specific transcription factor after asymmetric division. *Genes Dev* **17:** 1166–1174.
Fujita, M., and Losick, R. (2005) Evidence that entry into sporulation in *Bacillus subtilis* is governed by a gradual increase in the level and activity of the master regulator Spo0A. *Genes Dev* **19:** 2236–2244.
Fujita, M., González-Pastor, J.E., and Losick, R. (2005) High- and low-threshold genes in the Spo0A regulon of *Bacillus subtilis*. *J Bacteriol* **187:** 1357–1368.
Gholamhoseinian, A., Shen, Z., Wu, J.J., and Piggot, P. (1992) Regulation of transcription of the cell-division gene Ftsa during sporulation of *Bacillus-subtilis*. *J Bacteriol* **174:** 4647–4656.
Grossman, A.D. (1995) Genetic networks controlling the initiation of sporulation and the development of genetic competence in *Bacillus subtilis*. *Annu Rev Genet* **29:** 477–508.
Gueiros-Filho, F.J., and Losick, R. (2002) A widely conserved bacterial cell division protein that promotes assembly of the tubulin-like protein FtsZ. *Genes Dev* **16:** 2544–2556.
Hoch, J.A. (1993a) The phosphorelay signal transduction pathway in the initiation of *Bacillus subtilis* sporulation. *J Cell Biochem* **51:** 55–61.
Hoch, J.A. (1993b) Regulation of the phosphorelay and the initiation of sporulation in *Bacillus subtilis*. *Annu Rev Microbiol* **47:** 441–465.
de Jong, I.G., Veening, J.W., and Kuipers, O. (2010) Heterochronic phosphorelay gene expression as a source of heterogeneity in *Bacillus subtilis* spore formation. *J Bacteriol* **192:** 2053–2067.
Kobayashi, K., Shoji, K., Shimizu, T., Nakano, K., Sato, T., and Kobayashi, Y. (1995) Analysis of a suppressor mutation *ssb* (*kinC*) of *sur0B20* (*spo0A*) mutation in *Bacillus subtilis* reveals that *kinC* encodes a histidine protein-kinase. *J Bacteriol* **177:** 176–182.
Kuchina, A., Espinar, L., Cagatay, T., Balbin, A.O., Zhang, F., Alvarado, A., *et al*. (2011) Temporal competition between differentiation programs determines cell fate choice. *Mol Syst Biol* **7:** 557.
LeDeaux, J.R., and Grossman, A.D. (1995) Isolation and characterization of kinC, a gene that encodes a sensor kinase homologous to the sporulation sensor kinases KinA and KinB in *Bacillus subtilis*. *J Bacteriol* **177:** 166–175.
Levine, J.H., Fontes, M.E., Dworkin, J., and Elowitz, M.B. (2012) Pulsed feedback defers cellular differentiation. *PLoS Biol* **10:** e1001252.
Molle, V., Fujita, M., Jensen, S.T., Eichenberger, P., Gonzalez-Pastor, J.E., Liu, J.S., and Losick, R. (2003) The Spo0A regulon of *Bacillus subtilis*. *Mol Microbiol* **50:** 1683–1701.
Narula, J., Devi, S.N., Fujita, M., and Igoshin, O.A. (2012) Ultrasensitivity of the *Bacillus subtilis* sporulation decision. *Proc Natl Acad Sci USA* **109:** E3513–E3522.
Patrick, J.E., and Kearns, D.B. (2008) MinJ (YvjD) is a topological determinant of cell division in *Bacillus subtilis*. *Mol Microbiol* **70:** 1166–1179.
Pedrido, M.E., de Ona, P., Ramirez, W., Lenini, C., Goni, A., and Grau, R. (2013) Spo0A links de novo fatty acid synthesis to sporulation and biofilm development in *Bacillus subtilis*. *Mol Microbiol* **87:** 348–367.
Rudner, D.Z., and Losick, R. (2002) A sporulation membrane protein tethers the pro-sigmaK processing enzyme to its inhibitor and dictates its subcellular localization. *Genes Dev* **16:** 1007–1018.
Savageau, M.A. (1976) *Biochemical Systems Analysis: A Study of Function and Design in Molecular Biology*. Reading, MA: Addison-Wesley Pub. Co., Advanced Book Program.
Sliusarenko, O., Heinritz, J., Emonet, T., and Jacobs-Wagner, C. (2011) High-throughput, subpixel precision analysis of bacterial morphogenesis and intracellular spatio-temporal dynamics. *Mol Microbiol* **80:** 612–627.
Sonenshein, A. (2000) Control of sporulation initiation in *Bacillus subtilis*. *Curr Opin Microbiol* **3:** 561–566.
Soufo, C.D., Soufo, H.J., Noirot-Gros, M.F., Steindorf, A., Noirot, P., and Graumann, P.L. (2008) Cell-cycle-dependent spatial sequestration of the DnaA replication initiator protein in *Bacillus subtilis*. *Dev Cell* **15:** 935–941.
Sterlini, J.M., and Mandelstam, J. (1969) Commitment to sporulation in *Bacillus subtilis* and its relationship to development of actinomycin resistance. *Biochem J* **113:** 29–37.
Tatti, K.M., Carter, H.L., 3rd, Moir, A., and Moran, C.P., Jr (1989) Sigma H-directed transcription of *citG* in *Bacillus subtilis*. *J Bacteriol* **171:** 5928–5932.
Thomaides, H.B., Freeman, M., El Karoui, M., and Errington, J. (2001) Division site selection protein DivIVA of *Bacillus subtilis* has a second distinct function in chromosome segregation during sporulation. *Genes Dev* **15:** 1662–1673.
Wagner, J.K., Marquis, K.A., and Rudner, D.Z. (2009) SirA enforces diploidy by inhibiting the replication initiator DnaA during spore formation in *Bacillus subtilis*. *Mol Microbiol* **73:** 963–974.
Williams, C.L., and Cotter, P.A. (2007) Autoregulation is essential for precise temporal and steady-state regulation by the *Bordetella* BvgAS phosphorelay. *J Bacteriol* **189:** 1974–1982.

Williams, C.L., Boucher, P.E., Stibitz, S., and Cotter, P.A. (2005) BvgA functions as both an activator and a repressor to control Bvg phase expression of *bipA* in *Bordetella pertussis*. *Mol Microbiol* **56:** 175–188.

Wu, L.J., and Errington, J. (2003) RacA and the Soj-Spo0J system combine to effect polar chromosome segregation in sporulating *Bacillus subtilis*. *Mol Microbiol* **49:** 1463–1475.

Youngman, P., Zuber, P., Perkins, J.B., Sandman, K., Igo, M., and Losick, R. (1985) New ways to study developmental genes in spore-forming bacteria. *Science* **228:** 285–291.

Supporting information

Additional supporting information may be found in the online version of this article at the publisher's web-site.